JAAS

ROYAL SOCIETY OF CHEMISTRY

TECHNICAL NOTE

View Article Online
View Journal | View Issue

Open Access Article. Published on 25 March 2025. Downloaded on 1/22/2026 11:36:11 AM.
This article is licensed under a Creative Commons Attribution-NonCommercial 3.0 Unported Licence.

Check for updates

Cite this: *J. Anal. At. Spectrom.*, 2025, **40**, 1158

# Improving detection capabilities of biogenic selenium nanoparticles in spICP-MS using an anionic ion-exchange resin†

Nuria Guijarro-Ramírez, *[a] Iraide Sáez-Zamacona, [bc] Guillermo Grindlay, [a] Luis Gras [a] and Rosa María Martínez-Espinosa [bc]

Received 7th January 2025
Accepted 24th March 2025

DOI: 10.1039/d5ja00005j

rsc.li/jaas

Single particle inductively coupled plasma mass spectrometry (spICP-MS) is widely used for characterizing Se nanoparticles (SeNPs) biosynthesized by several microorganisms when exposed to Se oxyanions. However, characterization is challenging due to the high levels of dissolved ionic Se in cell culture media, particularly at short incubation times. This study demonstrates that employing an anionic ion-exchange resin (Amberlyst A-26) to remove dissolved Se species ($SeO_3^{2-}$ and $SeO_4^{2-}$) enhances the spICP-MS characterization of biogenic SeNPs. Extraction conditions were initially investigated (*i.e.*, resin amount, dissolved ionic Se concentration, extraction time and matrix effects), achieving quantitative removal of ionic Se without affecting nanoparticle concentration or size distribution. The resin treatment reduced the background signal by approximately eightfold and lowered the particle size detection limit ($LoD_{size}$) from >40 nm to 20 nm. This methodology was successfully used to characterize biogenic SeNPs produced by *H. mediterranei* at 24 and 60 h of incubation.

## 1. Introduction

Selenium nanoparticles (SeNPs) are employed in a wide range of applications due to their antibacterial, antioxidant and photoelectric properties, among others.[1–5] Biogenic SeNPs, produced by microorganisms exposed to Se oxyanions, offer an alternative to chemical synthesis and also enables coupling of bioremediation processes of metalloid-contaminated environments. Accurate characterization of SeNPs is essential in any of those areas for understanding nanomaterial behaviour and applicability. Single-particle inductively coupled plasma mass spectrometry (spICP-MS) has emerged as a powerful analytical tool for NP characterization due to its ability to provide not only information about chemical composition but particle size and particle concentration as well as to discriminate between dissolved and particulate forms of a given element. Characterization of SeNPs using spICP-MS faces significant obstacles due to low Se ionization efficiency and spectral interferences by polyatomic Ar-based species on major Se isotopes (*e.g.*, $^{40}Ar^{40}Ar^{+}/^{80}Se^{+}$). Nevertheless, Se detection capabilities can be greatly improved by using reaction cells with an appropriate gas ($H_2$, $O_2$, *etc.*).[6–8] On the other hand, SeNPs are highly labile nanomaterials prone to dissolving over time.[9–12] This phenomenon affects negatively both particle concentration and size limits of detection due to nanomaterial (NM) discrete signals that might not be easily discernible from the continuous background signal produced by Se dissolved ions.

When exposed to Se oxyanions, several microorganisms (*e.g.*, bacteria, fungi, algae, *etc.*) produce SeNPs with a mean particle diameter ranging from 30 to 300 nm.[1,9,13] In a recent study by our research group, a novel methodology was proposed to characterize biogenic SeNPs produced by the halophilic archaeon *Haloferax mediterranei* in brine samples (>150 g per L NaCl) containing $SeO_3^{2-}$ up to 80 mg $L^{-1}$.[14] By appropriate selection of experimental conditions and sample dilution ($1 \times 10^3$), both spectral and non-spectral interferences from sample concomitants are mitigated thus allowing accurate and precise characterization of biogenic SeNPs produced by *H. mediterranei*. However, this methodology was limited to samples incubated above 48 hours due to the high $SeO_3^{2-}$ concentration present in the early stages of the haloarchaeon growth that makes it impossible to differentiate SeNPs signals from Se dissolved background.[14] Though this issue might be overcome by an additional sample dilution step to reduce the ionic background ($>1 \times 10^3$), such approach would affect negatively the particle concentration limits of detection. So, alternative sample preparation strategies are desirable to investigate how SeNPs are produced by *H. mediterranei* over time as well as by any other

[a]*Department of Analytical Chemistry, Nutrition, and Food Sciences, University of Alicante, PO Box 99, 03080 Alicante, Spain. E-mail: nuria.guijarro@ua.es; guillermo.grindlay@ua.es*

[b]*Multidisciplinary Institute for Environmental Studies "Ramón Margalef", University of Alicante, Ap. 99, E-03080, Alicante, Spain*

[c]*Biochemistry, Molecular Biology, Edaphology and Agricultural Chemistry Department, Faculty of Sciences, University of Alicante, Ap. 99, E-03080 Alicante, Spain*

† Electronic supplementary information (ESI) available. See DOI: https://doi.org/10.1039/d5ja00005j

 This journal is © The Royal Society of Chemistry 2025

Open Access Article. Published on 25 March 2025. Downloaded on 1/22/2026 11:36:11 AM.
This article is licensed under a Creative Commons Attribution-NonCommercial 3.0 Unported Licence.

microorganisms capable of producing such NMs when exposed to Se or any other metals/metalloids.

To date, several strategies have been proposed to separate both SeNPs and Se dissolved fraction before spICP-MS analysis (capillary electrophoresis,[15] ultra-centrifugation with 10 kDa molecular weight cut-off filters,[16] field flow fractionation,[17] HPLC, *etc.*) but they are time-consuming and costly due to complex instrumental setup requirements. A possible solution may be the use of ion-exchange resins for selectively removing the Se dissolved fraction from the NM suspension. Both strong and weak cation exchange resins (Chelex® 100 resin and Dowex® 50 W-X8) have been successfully employed to reduce ionic background for characterizing metallic (Ag)[18] and metal oxide (ZnO, $Fe_2O_3$, $TiO_2$, *etc.*) NMs in wastewater samples.[19–24]

This study introduces a new procedure for characterizing SeNPs in complex samples containing high levels of salts and dissolved Se ($SeO_3^{2-}$ and $SeO_4^{2-}$) *via* spICP-MS following an anionic ion-exchange resin treatment. The ion exchange procedure was optimized by evaluating critical parameters, including resin quantity, elution volume, dissolved Se concentration and total dissolved solids content. The separation procedure was then applied to characterize biogenic SeNPs produced by *H. mediterranei* after of 24 and 60 hours of incubation.

# 2. Experimental

## 2.1. Reagents and microbial growth

A strong basic Amberlyst A26 hydroxide anion resin (Sigma-Aldrich, Madrid, Spain) was evaluated for separating SeNPs from Se oxyanions ($SeO_3^{2-}$ and $SeO_4^{2-}$) derived from $Na_2SeO_3$ and $Na_2SeO_4$ (Panreac, Barcelona, Spain). Selenium solutions were prepared using a 1000 mg per L Se standard (Sigma-Aldrich, Madrid, Spain) and a commercial SeNPs suspension (0.15 wt%, nominal size 153 ± 11 nm by transmission electron microscopy (TEM);[25] $5.5 \times 10^{13}$ SeNPs $L^{-1}$, Glantreo, Cork, Ireland). Cells culture media (minimal mineral medium, MMM) (Table S1†) were prepared with reagents: NaCl 99%, $MgCl_2 \cdot 6H_2O$ 99%, $MgSO_4 \cdot 7H_2O$ 99.5%, $CaCl_2 \cdot 6H_2O$ 98%, KCl 99%, $NaHCO_3$ 99.7%, Tris–HCl 99%, $NH_4Cl$ 99.5%, $K_2HPO_4$ 98%, $KH_2PO_4$ 99%, D-(+)-glucose 99.5%, $FeCl_3$ 97%, $Na_2SO_3$ 99%, $HNO_3$ 69%, NaOH 98% and $Na_2SO_3$ 99% from Panreac (Barcelona, Spain). All solutions were made with ultrapure water (Milli-Q, Millipore, Paris, France).

## 2.2. Instrumentation

An Agilent 8900 triple-quadrupole ICP-MS instrument (Santa Clara, USA) was employed through this work. Experimental conditions for SeNPs characterization were optimized elsewhere (Table S2†).[14] Briefly, because the most abundant Se isotope ($^{80}Se^+$) is severely interfered by $^{40}Ar^{40}Ar^+$, SeNPs were characterized using the collision-reaction cell in mass-shift mode ($^{80}Se^{16}O^+$). Nanomaterial transport efficiency was assessed by using the particle size methodology since it has been previously observed that it provides equivalents results to those obtained with the particle frequency approach when operating under optimum experimental conditions.[14]

## 2.3. Anion-exchange resin pretreatment

To remove dissolved Se ions present in SeNPs suspension, a strong basic anion resin (Amberlyst A-26) with a capacity 4.8 $m_{eq}\ g^{-1}$ was tested.[26] For resin pretreatment, 0.5 g of Amberlyst A-26 was preconditioned with 10 mL of 0.1 M NaOH and rinsed twice with 5 mL of ultrapure water per 0.5 g. Ten milliliters of sample (either SeNPs, dissolved Se, or a mixture) were then mixed directly with the preconditioned resin. The suspension was vortexed at 2000 rpm for 5 minutes and allowed to settle. Resin pearls settle quickly (<10 seconds) and the supernatant can be subsequently analyzed by ICP-MS.

To assess the possibility of reusing the resin, the retained Se was recovered by washing the resin twice with 5 mL of distilled water followed by a treatment with 3% (w/w) $HNO_3$, vortexing, and settling before analysis. The performance of the resin was estimated by calculating ionic Se retention (eqn (1)) and recovery (eqn (2)), as follows:

$$\text{Se retention capacity}(\%) = \frac{m_{\text{Initial Se}} - m_{\text{Final Se}}}{m_{\text{Initial Se}}} \times 100 \quad (1)$$

$$\text{Se recovery capacity}(\%) = \frac{m_{\text{Recovered Se}}}{m_{\text{Initial Se}}} \times 100 \quad (2)$$

where $m_{\text{Final Se}}$ is the remaining Se after the adsorption process, $m_{\text{Initial Se}}$ is the initial Se concentration, $m_{\text{Recovered Se}}$ is the ionic Se after the recovery process.

## 2.4. Characterization of biogenic SeNPs produced by *H. mediterranei*

The resin pretreatment was used to characterize biogenic SeNPs produced by *H. mediterranei*. Experiments were conducted using a strain R-4 (ATCC33500) (isolated from saltern ponds located in Santa Pola, Alicante, Spain)[27] cultured in a minimal mineral medium (MMM) (Table S1†)[14] containing 80 mg $L^{-1}$ of $SeO_3^{2-}$. After 24 and 60 hours, 1 mL aliquots were collected and transferred to microcentrifuge tubes. Because total dissolved solids (TDS) and SeNPs concentration levels are high and they could negatively affect data accuracy and precision (*e.g.*, non-spectral interferences, double signal events, *etc.*),[14] samples were diluted ($1 \times 10^3$–$1 \times 10^5$) before the anion-exchange resin treatment and spICP-MS characterization.

# 3. Results and discussion

## 3.1. Optimization of resin operating conditions

After checking previous studies in the literature[18,19,26] and conducting some preliminary experiments, the following parameters were selected for methodology optimization: (i) Se dissolved concentration; (ii) extraction time; and (iii) resin quantity. Preliminary tests using $SeO_3^{2-}$ standards (0.1–1 mg $L^{-1}$) showed quantitative Se retention when 10 mL of solution was mixed with 0.5 g of resin for 5 minutes (Fig. S1A†). Although extraction times between 5 and 30 minutes yielded similar retention efficiencies (99.3–99.9%), a 5-minute extraction was

Open Access Article. Published on 25 March 2025. Downloaded on 1/22/2026 11:36:11 AM.
This article is licensed under a Creative Commons Attribution-NonCommercial 3.0 Unported Licence.

selected to maximize sample throughput. Further experiments revealed that resin masses above 0.3 g ensured complete Se uptake; however, to account for competitive binding from other anions present in *H. mediterranei* media, 0.5 g was deemed optimal (Fig. S1B†). To extend the applicability of the proposed method to a broader range of scenarios, it was investigated whether it could also be applied to remove other Se-dissolved species such as $SeO_4^{2-}$. To this end, a 1000 μg per L $SeO_4^{2-}$ was mixed with 0.5 g of the resin for 5 minutes and subsequently analyzed by analyzed by ICP-MS. It was observed that $SeO_4^{2-}$ was quantitatively retained thus confirming that this strategy can be employed for different Se dissolved species. No further experiments were carried out with $SeO_4^{2-}$ since *H. mediterranei* does not produce SeNPs in the presence of this compound.[14] In addition, recovery experiments using a 3% $HNO_3$ eluent indicated that a 10 mL volume was necessary to quantitatively recover the retained Se, with the resin demonstrating consistent performance over five reuse cycles (RSD = 1.8%; see Fig. S1C†).

### 3.2. Influence of the ion-exchange resin treatment on SeNPs characterization

Several authors have noticed that ion-exchange resins do not only interact with dissolved ions but with NMs. Though that interaction is not so strong, may bias particle concentration data.[28,29] For this reason, the influence of the ion-exchange resin treatment on SeNPs characterization was checked. Prior to spICP-MS analysis, after the resin treatment the resin rapidly sedimented, the supernatant was carefully separated, and the resulting dilutions were ultrasonicated for 1 minute to ensure complete nanoparticle resuspension and minimize agglomeration. spICP-MS analysis revealed that the particle concentration was virtually identical before ((2.93 ± 0.12) × $10^7$ particles per mL) and after ((2.92 ± 0.16) × $10^7$ particles per mL) treatment. Moreover, the particle size distribution remained unchanged (Fig. 1), confirming that the resin treatment does not alter the physical characteristics of the SeNPs. These results strongly support the use of the anionic resin for selective removal of dissolved Se without compromising nanoparticle integrity.

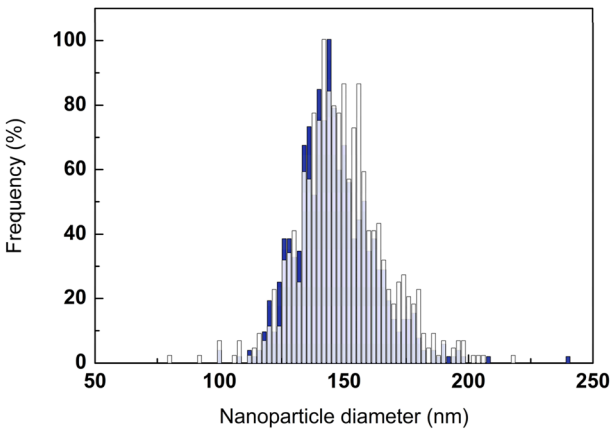


Fig. 1 Size distribution of a commercial dispersion of SeNPs (nominal size 153 ± 11 nm) measured with (■) and without (■) the resin treatment. Experimental conditions: resin mass: 0.5 mg; extraction time: 5 min.

### 3.3. Matrix effects

Culture growth media for haloarchaea contain a wide range of salt and organic species which might negatively affect $SeO_3^{2-}$ extraction by the resin. In fact, TDS content of *H. mediterranei* MMM (242 g $L^{-1}$) (Table S1†) is particularly higher than typical media (*e.g.*, Luria–Bertani, 20 g $L^{-1}$). To assess matrix effects, *H. mediterranei* MMM was initially diluted 1 × $10^2$, 1 × $10^3$ and 1 × $10^6$ times. Each dilution corresponds to a final TDS content of 2, 0.2 and 2 × $10^{-4}$ g $L^{-1}$, respectively. Next, samples were spiked with 1 mg per L $SeO_3^{2-}$ and treated with the ion-exchange resin for $SeO_3^{2-}$ removal. Dilutions below 1 × $10^2$ were avoided since the high salt content affects negatively instrument performance[14] and a minimum dilution is needed to lyse *H. mediterranei* by osmotic shock, preventing intracellular $SeO_3^{2-}$/SeNP bioaccumulation. As shown in Fig. S2,† $SeO_3^{2-}$ retention was quantitative for a concentration of TDS up to 0.2 g $L^{-1}$ whereas above that level diminished (92 ± 3%). Considering that the Amberlyst A26 resin has a capacity of 4.8 $m_{eq}$ $g^{-1}$ and that the medium contains approximately 107 g $L^{-1}$ of $Cl^-$, different water dilutions result in different chlorine concentrations: 1.07 g $L^{-1}$, 1.07 × $10^{-1}$ g $L^{-1}$, and 1.07 × $10^{-4}$ g $L^{-1}$. At the lowest dilution (2 g per L TDS, of which 1.07 g $L^{-1}$ is $Cl^-$), the ionic load corresponds to approximately 0.3 $m_{eq}$, representing about 13% of the total capacity of the resin. A similar reasoning applies to other anions present in the medium (*e.g.*, sulphate or phosphate). This aligns with the observed reduction in Se retention at 2 g per L TDS, confirming that higher TDS levels reduce retention efficiency due to competition between $Cl^-$ (or any other abundant anion) and $SeO_3^{2-}$ for the exchange sites of the resin. It is expected that at lower dilutions, the capacity of the resin would be even further compromised. Anyway, the high tolerance of the Amberlyst A26 resin to matrix concomitants present in MMM means that it could be employed for characterizing biogenic SeNPs present in non-hypersaline media applications. From these results, the maximum concentration of TDS tolerable for the resin was established at 0.2 g $L^{-1}$ (1 × $10^3$ dilution). Interestingly, it was already observed in our previous work that plasma matrix effects for that dilution are minimum which allow to calibrate with water standards.[14] So, the ion-exchange pretreatment can be directly implemented to our existing analytical protocol without any additional modification.

To evaluate the potential benefits of $SeO_3^{2-}$ removal on SeNPs characterization, *H. mediterranei* cell growth media containing 80 mg $L^{-1}$ of $SeO_3^{2-}$ (*i.e.* no cells/NPs) was diluted 1 × $10^3$ and analyzed by means of spICP-MS with and without the resin treatment (Fig. S3†). The results showed that $^{80}Se^{16}O^+$ signal decreased by approximately 98% after the resin treatment (resin: 1.1 × $10^3$ cps; no resin: 4.8 × $10^5$ cps). Consequently, the baseline equivalent diameter (BED) was reduced from 100 nm before treatment to 25 nm, representing a decrease of up to 75%. This decrease in the BED is consistent with previous reports and clearly highlights the benefits of

 This journal is © The Royal Society of Chemistry 2025

Open Access Article. Published on 25 March 2025. Downloaded on 1/22/2026 11:36:11 AM.
This article is licensed under a Creative Commons Attribution-NonCommercial 3.0 Unported Licence.

using resin treatments for NMs characterization.[19] Finally, it is important to highlight that the proposed method is beneficial in terms of sample throughput and simplicity. Resins are directly introduced into the sample and, after 5 minutes, NMs suspension can be directly analyzed without the practical shortcomings associated with solid-phase extraction (*e.g.*, column swelling or shrinking, high back pressure due to tighter packing of the column material, *etc.*).[30]

### 3.4. Real sample analysis

The proposed methodology was applied to characterize SeNPs produced by *H. mediterranei* exposed to 80 mg $L^{-1}$ of $SeO_3^{2-}$. Cell growth media aliquots of 1 mL were collected at 0, 24 and 60 hours, covering different scenarios of $SeO_3^{2-}$ levels. Next, aliquots were diluted to reduce TDS content below 0.2 g $L^{-1}$ as well as to lysate the cells. Because *H. mediterranei* is highly efficient in producing SeNPs, a $1 \times 10^5$ dilution was employed instead of a $1 \times 10^3$ one to mitigate the potential occurrence of double events. In fact, when using the latter dilution, more than 50 000 events were observed for samples incubated 24 and 60 h thus giving rise to biased results.[14] The diluted aliquots were analyzed by spICP-MS both directly and after treatment with an ion-exchange resin.

Fig. 2 shows $^{80}Se^{16}O^+$ time scans with and without the resin treatment for the *H. mediterranei* cell cultures incubated for 0, 24 and 60 h. For direct sample analysis (*i.e.*, no resin treatment), Se dissolved background signal decreased 1.5-fold with time (0/24 h: $8.0 \times 10^3$ cps; 48 h: $5.6 \times 10^3$ cps) whereas both the number of pulses and pulse intensity increased. In contrast, resin-treated samples exhibited a constant background (0/24/48 h: $1.0 \times 10^3$ cps), about 8 times lower than in direct sample analysis. Interestingly, background signal after the resin treatment was equivalent to that previously obtained for the $1 \times 10^3$ solution. This background reduction is beneficial to distinguish NMs signal pulses from the background thus improving detection capabilities and NMs characterization accuracy since the analysis is independent on the $SeO_3^{2-}$ levels present in the culture medium. In fact, particle size detection limit ($LoD_{size}$) without the resin treatment was critically dependent on the incubation time (*i.e.*, Se dissolved levels), ranging from 45 (24 h) to 40 nm (60 h), while resin treatment consistently yielded a $LoD_{size}$ of 20 nm. Particle concentration limit of detection ($LOD_{conc}$) was calculated for both approaches[31] (dilution $1 \times 10^5$) providing similar values around $8 \times 10^7$ particles per mL. Nevertheless, because there is no limitation to operate the resin using a $1 \times 10^3$ dilution, the latter approach is indeed beneficial for improving $LOD_{conc}$ ($2 \times 10^5$ particles per mL) regarding the direct analysis without the resin (Fig. S3†). Table S3† shows particle concentration and particle mean size for SeNPs incubated 24 h and 60 h. As expected from our previous work, both particle mean size and concentration increased with time. Irrespective of the sample preparation treatment,[14] no significant differences were observed on both parameters for an incubation time of 60 h due to a significant amount of the $SeO_3^{2-}$ has transformed into SeNPs and the average NMs size was far beyond the methodology limits of detection. In fact, particle size mean diameter data agreed with the results

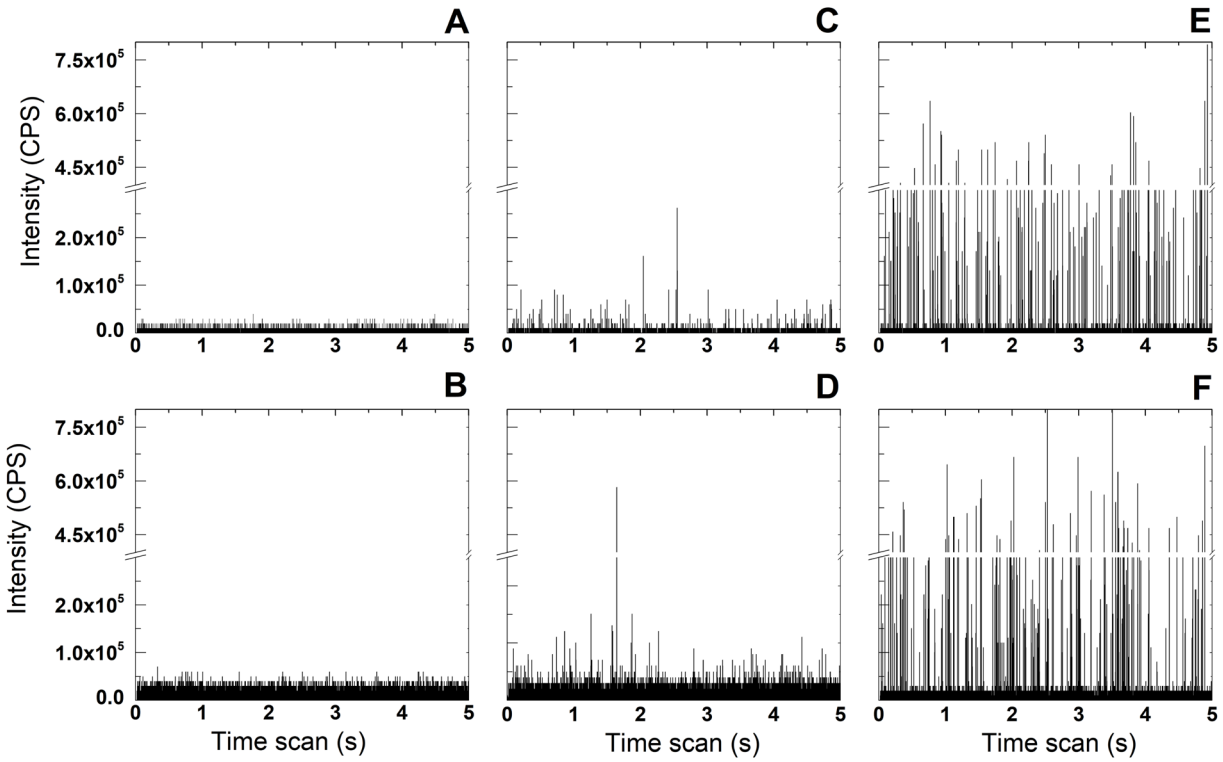


Fig. 2 $^{80}Se^{16}O^+$ time scan for $1 \times 10^5$ diluted *H. mediterranei* cell growth media with and without the resin treatment at different incubation times. (A) 0 h, resin; (B) 0 h, no resin; (C) 24 h, resin; (D) 24 h, no resin; (E) 60 h, resin; and (F) 60 h, no resin.

Open Access Article. Published on 25 March 2025. Downloaded on 1/22/2026 11:36:11 AM.
This article is licensed under a Creative Commons Attribution-NonCommercial 3.0 Unported Licence.

obtained using TEM. However, there were significant differences on both parameters for the sample incubated at 24 h. Thus, particle mean size with and without the resin treatment were 65.0 ± 0.1 and 71.6 ± 0.1 nm, respectively. Interestingly, the average size with TEM was 63 ± 3 nm. As regards particle concentration, experimental values for the resin treatment ((3.7 ± 0.1) × $10^{12}$ particles per mL) were slightly higher than those for direct analysis ((3.1 ± 0.4) × $10^{12}$ particles per mL). To explain these findings, it should be considered that $SeO_3^{2-}$ ionic background signal reduction makes easier to identify signal pulses. Consequently, the number of events with the resin treatment was higher and particle size distributions were displaced to lower particle size values. These results clearly highlight the benefits of using anionic exchange-resins for characterizing SeNPs produced by *H. mediterranei* when $SeO_3^{2-}$ levels in solution are significant.

## 4. Conclusions

This work demonstrates that Amberlyst A-26 (strong basic anionic exchange-resin) effectively reduces background signals from Se dissolved species in spICP-MS. Using 0.5 g of resin for 5 minutes of extraction time, both $SeO_3^{2-}$ and $SeO_4^{2-}$ are quantitatively removed thus allowing accurate and precise SeNPs characterization. For solutions with TDS > 2 × $10^{-1}$ g $L^{-1}$, sample dilution is required to ensure Se dissolved species removal. The proposed methodology was successfully applied to characterize SeNPs produced by the archaeon *H. mediterranei*, particularly at short incubation times when selenite levels are significant. It is expected that this approach can also be applied to the analysis of biogenic SeNPs generated by other microorganisms where Se dissolved content may interfere with spICP-MS determinations and provide insights into the temporal evolution of SeNP production, especially during early incubation stages.

## Data availability

Data will be made available on request.

## Conflicts of interest

There are no conflicts to declare.

## Acknowledgements

The authors would like to thank the Generalitat Valenciana (PROMETEO/2021/055), Vicerrectorado de Investigación de la Universidad de Alicante (VIGROB-050 and VIGROB-309) and Ministerio de Economía y Empresa del Gobierno de España (eqn C2018-004065-P) for the financial support of this work.

## References

1 N. Bisht, P. Phalswal and P. K. Khanna, *Mater. Adv.*, 2022, **3**, 1415–1431.
2 T. Liang, X. Qiu, X. Ye, Y. Liu, Z. Li, B. Tian and D. Yan, *3 Biotech*, 2020, **10**, 23.
3 S. Sampath, V. Sunderam, M. Manjusha, Z. Dlamini and A. V. Lawrance, *Molecules*, 2024, **29**, 801.
4 T. Ramachandran, D. Manoharan, S. Natesan, S. K. Rajaram, P. Karuppiah, M. R. Shaik, M. Khan and B. Shaik, *Biomedicines*, 2023, **11**, 2520.
5 Y. Huang, E. Su, J. Ren and X. Qu, *Nano Today*, 2021, **38**, 101205.
6 B. M. Freire, Y. T. Cavalcanti, C. N. Lange, J. C. Pieretti, R. M. Pereira, M. C. Gonçalves, G. Nakazato, A. B. Seabra and B. L. Batista, *Nanotechnology*, 2022, **33**, 355702.
7 K. C. Nwoko, X. Liang, M. A. Perez, E. Krupp, G. M. Gadd and J. Feldmann, *J. Chromatogr. A.*, 2021, **1642**, 462022.
8 R. Álvarez-Fernández García, M. Corte-Rodríguez, M. Macke, K. L. LeBlanc, Z. Mester, M. Montes-Bayón and J. Bettmer, *Analyst*, 2020, **145**, 1457–1465.
9 T. Zhang, M. Qi, Q. Wu, P. Xiang, D. Tang and Q. Li, *Front. Nutr.*, 2023, **10**, 1183487.
10 H. He, C. Liu, C. Shao, Y. Wu and Q. Huang, *Mater. Lett.*, 2022, **317**, 132079.
11 D. Torregrosa, G. Grindlay, L. Gras and J. Mora, *J. Anal. At. Spectrom.*, 2023, **38**, 1874–1884.
12 C. Gómez-Pertusa, M. C. García-Poyo, G. Grindlay, R. Pedraza, M. A. Yáñez and L. Gras, *Talanta*, 2024, **272**, 125742.
13 S. A. Wadhwani, U. U. Shedbalkar, R. Singh and B. A. Chopade, *Appl. Microbiol. Biotechnol.*, 2016, **100**, 2555–2566.
14 N. Guijarro-Ramírez, I. Sáez-Zamacona, D. Torregrosa, G. Grindlay, L. Gras, R. M. Martínez-Espinosa, C. Pire and J. Mora, *Anal. Chim. Acta*, 2025, **1335**, 343453.
15 F. Grønbæk-Thorsen, R. H. Hansen, J. Østergaard, B. Gammelgaard and L. H. Møller, *Anal. Bioanal. Chem.*, 2021, **413**, 2247–2255.
16 M. Palomo-Siguero, P. Vera, Y. Echegoyen, C. Nerin, C. Cámara and Y. Madrid, *Spectrochim. Acta, Part B*, 2017, **132**, 19–25.
17 L. Maknun, J. Sumranjit and A. Siripinyanond, *RSC Adv.*, 2020, **10**, 6423–6435.
18 M. Iglesias and L. Torrent, *Nanomaterials*, 2021, **11**, 2626.
19 K.-B. Yoo, S. Yang, H. Choi and B.-T. Lee, *Environ. Sci. Pollut. Res.*, 2024, **31**, 53090–53099.
20 P. Cervantes-Avilés and A. A. Keller, *Water Res.*, 2021, **189**, 116603.
21 A. Azimzada, N. Tufenkji and K. J. Wilkinson, *Environ. Sci.:Nano*, 2017, **4**, 1339–1349.
22 M. Hadioui, C. Peyrot and K. J. Wilkinson, *Anal. Chem.*, 2014, **86**, 4668–4674.
23 L. Fréchette-Viens, M. Hadioui and K. J. Wilkinson, *Talanta*, 2019, **200**, 156–162.
24 P. Cervantes-Avilés, Y. Huang and A. A. Keller, *Water Res.*, 2019, **166**, 115072.
25 A. Vladár and V.-D. Hodoroaba, Characterization of nanoparticles by scanning electron microscopy, in *Characterization of Nanoparticles*, Elsevier, 2020, ch. 2.1.1, pp. 7–27.
26 K. Pyrzyńska, *Analyst*, 1995, **120**, 1933–1936.

 This journal is © The Royal Society of Chemistry 2025

Open Access Article. Published on 25 March 2025. Downloaded on 1/22/2026 11:36:11 AM.
This article is licensed under a Creative Commons Attribution-NonCommercial 3.0 Unported Licence.

27 I. Saez-Zamacona, G. Grindlay and R. M. Martínez-Espinosa, *Mar. Drugs*, 2023, **21**, 72.
28 H. M. Pouran, V. Llabjani, F. L. Martin and H. Zhang, *Environ. Sci. Technol.*, 2013, **47**, 11115–11121.
29 H. Pouran, R. Perez Colodrero, S. Wu, G. Hix, J. Zakharova and H. Zhang, *Anal. Methods*, 2020, **12**, 959–969.
30 J. Wang and E. H. Hansen, *TrAC, Trends Anal. Chem.*, 2003, **22**, 836–846.
31 F. Laborda, E. Bolea and J. Jiménez-Lamana, *Anal. Chem.*, 2014, **86**, 2270–2278.